Transplanted Mesenchymal Stem Cells Reduce Autophagic Flux in Infarcted Hearts via the Exosomal Transfer of miR-125b

Changchen Xiao, Kan Wang, Yinchuan Xu, Hengxun Hu, Na Zhang, Yingchao Wang, Zhiwei Zhong, Jing Zhao, Qingju Li, Dan Zhu, Changle Ke, Shuhan Zhong, Xianpeng Wu, Hong Yu, Wei Zhu, Jinghai Chen, Jianyi Zhang, Jian'an Wang, Xinyang Hu

Rationale: **Autophagy can preserve cell viability under conditions of mild ischemic stress by degrading damaged organelles for ATP production, but under conditions of severe ischemia, it can promote cell death and worsen cardiac performance. Mesenchymal stem cells (MSCs) are cardioprotective when tested in animal models of myocardial infarction, but whether these benefits occur through the regulation of autophagy is unknown.**

Objective: **To determine whether transplanted MSCs reduce the rate of autophagic degradation (autophagic flux) in infarcted hearts and if so, to characterize the mechanisms involved.**

Methods and Results: **Treatment with transplanted MSCs improved cardiac function and infarct size while reducing apoptosis and measures of autophagic flux (bafilomycin A1-induced LC3-II [microtubule-associated protein 1 light chain 3] accumulation and autophagosome/autolysosome prevalence) in infarcted mouse hearts. In hypoxia and serum deprivation–cultured neonatal mouse cardiomyocytes, autophagic flux and cell death, as well as p53-Bnip3 (B-cell lymphoma 2–interacting protein 3) signaling, declined when the cells were cultured with MSCs or MSC-secreted exosomes (MSC-exo), but the changes associated with MSC-exo were largely abolished by pretreatment with the exosomal inhibitor GW4869. Furthermore, a mimic of the exosomal oligonucleotide miR-125b reduced, whereas an anti-miR-125b oligonucleotide increased, autophagic flux and cell death, via modulating p53-Bnip3 signaling in hypoxia and serum deprivation–cultured neonatal mouse cardiomyocytes. In the in vivo mouse myocardial infarction model, MSC-exo, but not the exosomes obtained from MSCs pretreated with the anti-miR-125b oligonucleotide (MSC-exo$^{anti\text{-}miR\text{-}125b}$), recapitulated the same results as the in vitro experiments. Moreover, measurements of infarct size and cardiac function were significantly better in groups that were treated with MSC-exo than the MSC-exo$^{anti\text{-}miR\text{-}125b}$ group.**

Conclusions: **The beneficial effects offered by MSC transplantation after myocardial infarction are at least partially because of improved autophagic flux through excreted exosome containing mainly miR-125b-5p. (*Circ Res*. 2018;123:564-578. DOI: 10.1161/CIRCRESAHA.118.312758.)**

Key Words: autophagy ■ mesenchymal stromal cells ■ microRNAs ■ myocardial infarction ■ stem cells

Bone marrow mesenchymal stem cells (MSCs) are among the most common types of cells used for investigations of myocardial cell therapy, because they are relatively easy to obtain, highly proliferative, anti-inflammatory, and only mildly immunogenic.[1] Previous studies have shown that the improvements in infarct size and heart function observed when MSCs are transplanted into hearts after acute myocardial infarction (MI) or ischemia-reperfusion injury are accompanied by declines in cardiomyocyte death,[2,3] and these cardioprotective effects are mediated by paracrine factors.[3–7] Exosomes are cell-derived microvesicles that facilitate intracellular communication and can regulate cell fate by transferring a variety

Editorial, see p 518
In This Issue, see p 507
Meet the First Author, see p 508

Original received January 21, 2018; revision received June 3, 2018; accepted June 18, 2018. In May 2018, the average time from submission to first decision for all original research papers submitted to *Circulation Research* was 13.37 days.

From the Department of Cardiology, Second Affiliated Hospital, College of Medicine (C.X., K.W., Y.X., H.H., N.Z., Y.W., Z.Z., J.Z., Q.L., D.Z., C.K., S.Z., X.W., H.Y., W.Z., J.C., J.W., X.H.) and Institute of Translational Medicine (J.C.), Zhejiang University, Hangzhou, China; Cardiovascular Key Laboratory of Zhejiang Province, Hangzhou, China (C.X., K.W., Y.X., H.H., N.Z., Y.W., Z.Z., J.Z., Q.L., D.Z., C.K., S.Z., X.W., H.Y., W.Z., J.C., J.W., X.H.); and Department of Biomedical Engineering, University of Alabama at Birmingham (J.Z.).

The online-only Data Supplement is available with this article at https://www.ahajournals.org/doi/suppl/10.1161/CIRCRESAHA.118.312758.

Correspondence to Xinyang Hu, MD, PhD, Department of Cardiology, Provincial Key Laboratory of Cardiovascular Research, Second Affiliated Hospital, College of Medicine, Zhejiang University, Hangzhou 310009, China. Email hxy0507@zju.edu.cn; or Jian'an Wang, MD, PhD, Department of Cardiology, Provincial Key Laboratory of Cardiovascular Research, Second Affiliated Hospital, College of Medicine, Zhejiang University, Hangzhou 310009, China, Email wangjianan111@zju.edu.cn

Novelty and Significance

What Is Known?

- Mesenchymal stem cells (MSCs) are frequently used for investigative cell-based myocardial therapies.
- MSC-derived exosomes play an important role in the paracrine activity of MSCs.
- Autophagy can be an adaptive response that preserves cell viability under conditions of mild ischemic stress, but if the ischemic event is more severe, autophagic activity (ie, autophagic flux) increases, which promotes cell death and exacerbates myocardial dysfunction.

What New Information Does This Article Contribute?

- MSCs inhibit autophagic flux and reduce cell death when transplanted into the hearts of mice after myocardial infarction.
- The decline in autophagic flux associated with MSC transplantation is mediated by exosomes.
- The antiautophagic component of the MSC exosomal cargo is miR-125b-5p, which interferes with p53/Bnip3 (B-cell lymphoma 2–interacting protein 3) signaling.

Autophagy is an evolutionarily conserved process by which cytosolic proteins and subcellular structures are degraded and recycled for ATP production and protein synthesis. Under conditions of mild ischemic stress, autophagy can be an adaptive response that preserves cell viability, but when the ischemic event is more severe, autophagic flux increases and could promote cell death, thereby worsening cardiac performance. Here, we show that at least some of the benefits associated with MSC transplantation after myocardial infarction in mice are related to a decline in ischemia-induced autophagic flux and that this effect is mediated by the exosomal transfer of miR-125b-5p from MSCs to the native cells.

Nonstandard Abbreviations and Acronyms

3-MA	3-methyladenine
AMPK	5′-adenosine monophosphate–activated protein kinase
BafA1	bafilomycin A1
Bnip3	B-cell lymphoma 2–interacting protein 3
CD	cluster of differentiation
GFP	green fluorescent protein
H/SD	hypoxia and serum deprivation
MI	myocardial infarction
MSC	mesenchymal stem cell
MSC-exo	mesenchymal stem cell–secreted exosome
NC	negative control
NMCM	neonatal mouse cardiomyocyte
RFP	red fluorescent protein

of proteins and oligonucleotides between cells.[8–10] It has been known that exosomes play key roles in the paracrine actions of MSCs, thereby exerting the myocardial protective effects in the setting of MI and ischemia/reperfusion injury; however, the cardioprotective component of the cargo of MSC-derived exosomes has yet to be identified.

Autophagy is an evolutionarily conserved process by which long-lived cytosolic proteins and damaged organelles are degraded and recycled for ATP production and protein synthesis.[11–13] Under conditions of mild ischemia, autophagy can be an adaptive response that preserves cell viability, limits infarct size, and attenuates adverse left ventricular remodeling.[14–16] However, if the ischemic event is more severe or prolonged, the autophagic process may become chronically activated, leading to increases of cell death, including the death of cardiomyocytes,[14,17,18] and declines in myocardial function.[19] However, whether autophagy is involved in the cardioprotection of stem cell therapy and what is the regulation mechanism remain unclear. Here, we present the results from a series of in vivo and in vitro experiments designed to determine whether the cardioprotective effects associated with MSC transplantation after MI are mediated by exosomes and induced, at least in part, via changes in the autophagic response to ischemia.

Methods

The authors declare that all data that support the findings of this study are available within the article and its Online Data Supplement.

A more detailed description of the experimental methods is available in the Online Data Supplement.

Animals

Experiments involving live animals were performed in accordance with the Guide for the Care and Use of Laboratory Animals published by the US National Institutes of Health (National Institutes of Health publication No. 85-23, revised 1996) and were approved by the Institutional Animal Care and Use Committee of Zhejiang University. Male C57BL/6J mice (8–12 weeks old) and neonatal male C57BL/6J mice were purchased from Shanghai Slac Laboratory Animal Technology Corporation, and both male and female CAG-RFP-EGFP-LC3 transgenic C57BL/6J mice (CAG [cytomegalovirus immediate early promoter enhancer with chicken beta-actin/rabbit beta-globin hybrid promoter]-RFP [red fluorescent protein]-EGFP [enhanced green fluorescent protein]-LC3, stock No. 027139) were purchased from the Jackson Laboratories (Bar Harbor, ME). The animals were fed a standard laboratory diet and maintained within a 12:12-hour light/dark cycle.

Statistical Analysis

All data were reported as the mean±SE. The Student *t* test was performed to compare 2 groups, comparisons among ≥3 groups were evaluated via 1-way ANOVA followed by Bonferroni multiple comparison test, and comparisons among groups after multiple treatments were evaluated via 2-way ANOVA followed by Bonferroni multiple comparison test. $P<0.05$ was considered statistically significant. Statistical calculations were performed using GraphPad Prism 6.0.

Results

MSC Administration After MI Improves Heart Function and Protects Against Cardiac Cell Death

Whether MSC transplantation improves myocardial recovery after ischemic injury by modulating autophagic activity was investigated in a murine MI model. As reported previously,[20] measurements of infarct size (Online Figure IIA and IIB) and cardiac function (Online Figure IIC through IIG), as well as apoptosis in the border zone of ischemia (Online Figure IIH

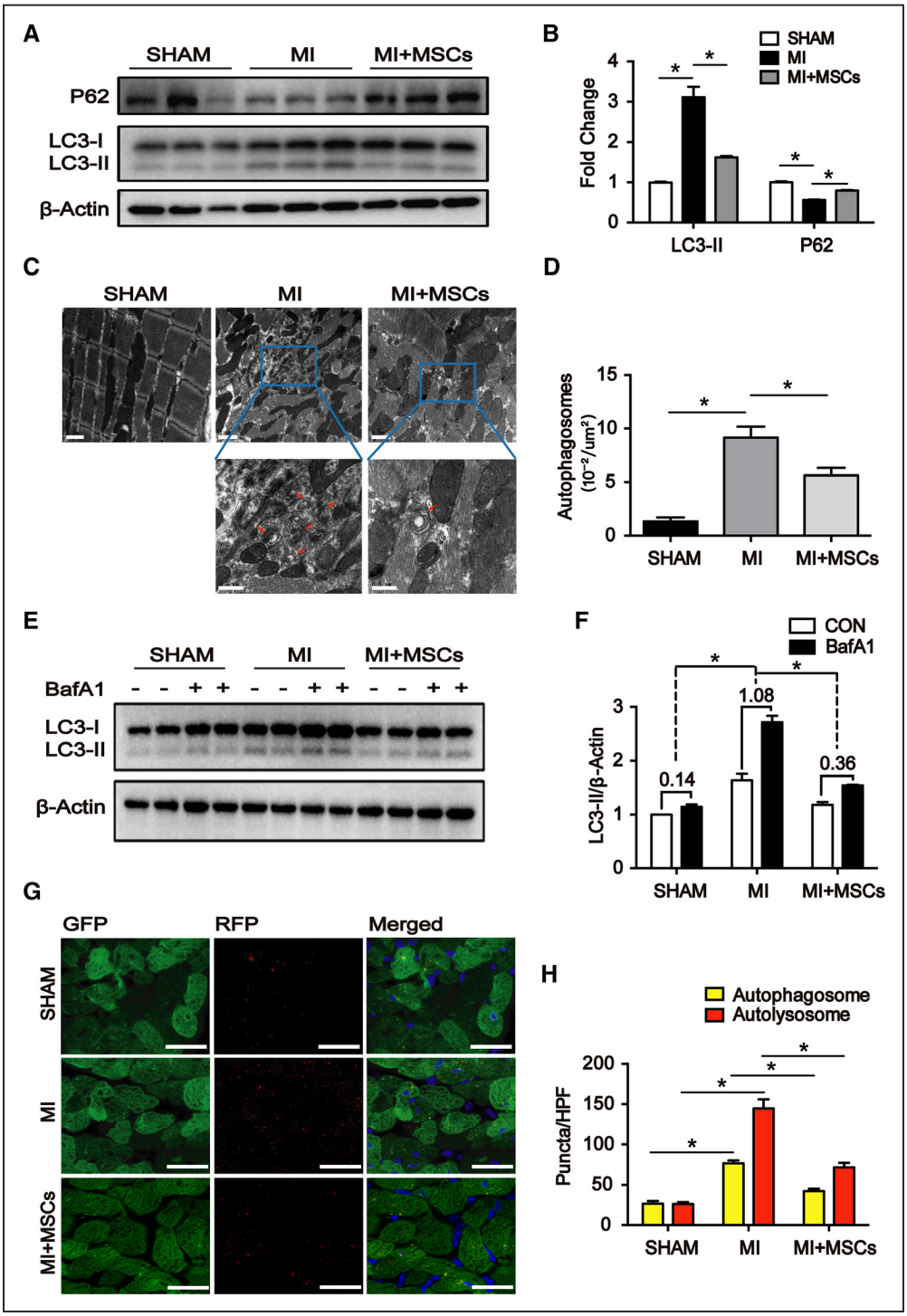

Figure 1. Mesenchymal stem cell (MSC) delivery inhibits autophagic flux after myocardial infarction. A and **B**, Autophagy protein expressions including P62 and LC3-II (microtubule-associated protein 1 light chain 3) were evaluated in sham-operated mice and coronary ligated mice that either received no therapy or MSC transplantation 24 h after myocardial infarction (MI; n=9 per group). Western blot analysis of protein lysates harvested from infarct border zone. Quantitative analysis of P62 and LC3-II is shown in (**right**). **C** and **D**, Autophagosomes were detected (**left**) and quantified (**right**) by TEM for each group of mice 24 h after MI within the border zone. Arrowhead, autophagosomes (n=3–4 per group; scale bars=1 um in [**top**] and 0.5 um in [**bottom**], respectively). **E** and **F**, Autophagic flux was evaluated with bafilomycin A1 (BafA1) used in each group of mice as described above. BafA1 (1.5 mg/kg) was injected intraperitoneally 2 h before sacrifice. LC3 levels were evaluated again by Western blotting for infarct border zone at 24 h after in the absence or presence of BafA1 intervention. LC3-II expression levels both before and after BafA1 intervention were quantified, and their absolute changes (indicating autophagic flux) were calculated and analyzed by 1-way ANOVA shown in (**right**; n=6 per group). **G** and **H**, Representative fluorescence images of heart tissue sections were obtained at 24 h in infarct border zone after MI from CAG (cytomegalovirus immediate early promoter enhancer with chicken beta-actin/rabbit beta-globin hybrid promoter)-RFP (red fluorescent protein)-EGFP (enhanced green fluorescent protein)-LC3 transgenic mice that were exposed to MI or MI with MSC transplantation. Autophagosome (yellow puncta) and autolysosome (red puncta) numbers in heart were calculated respectively (n=3–4 per group with 4–5 microscopic fields per heart section analyzed; scale bar=25 μm). Quantification is shown in the (**right**). HPF indicates high-power field. *P<0.05.

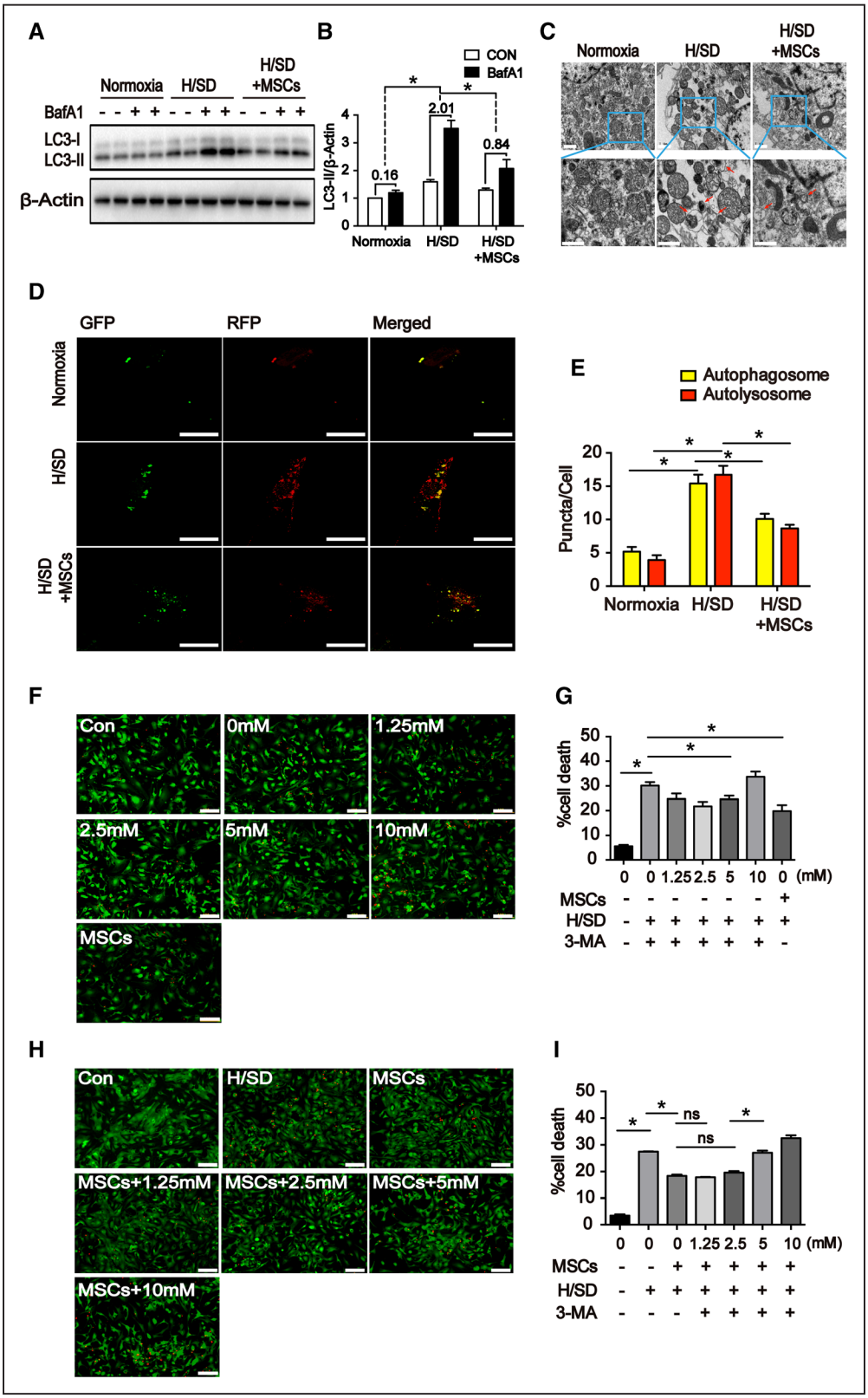

Figure 2. Mesenchymal stem cell (MSC) coculture inhibits autophagic flux and reduces cell death. A and **B**, LC3-II (microtubule-associated protein 1 light chain 3) levels were evaluated by Western blotting in 24-h hypoxia and serum deprivation (H/SD)–exposed neonatal mouse cardiomyocytes (NMCMs) with or without MSC coculture, and bafilomycin A1 (BafA1) was also used to evaluate the autophagic flux (n=3 independent experiments). LC3-II expression levels both before and after BafA1 intervention were quantified, and their absolute changes (indicating autophagic flux) were calculated and analyzed by 1-way ANOVA shown in (**right**). **C**, Autophagosomes in 24-h H/SD-exposed NMCMs with or without MSC coculture were detected by TEM. Arrowhead, autophagosomes and autolysosomes (scale bar=1 μm). **D** and **E**, Autophagosomes (yellow) and autolysosomes (red) were detected in 24-h H/SD exposed NMCMs expression mRFP (mCherry red fluorescent protein)-GFP (green fluorescent protein)-LC3 with or without MSC coculture (scale bar=25 μm). Numbers of autophagosomes and autolysosomes in each cell (20–30 cells per group) (*Continued*)

Figure 2 Continued. were quantified (n=3 independent experiments). **F** and **G**, The effects of autophagy on the survival of 24-h H/SD-exposed NMCMs were evaluated using different doses of 3-methyladenine (3-MA) compared with normoxia-treated NMCMs, and the beneficial effects of MSC coculture were also assayed. Fluorescence staining with vital dyes Calcein acetoxymethyl (Calcein-AM) shown in green indicates live cells, whereas ethidium homodimer-1 staining shown in red indicates the dead cells. The percentage of cell death is shown in (**right**; n=3 independent experiments). **H** and **I**, The effects of autophagy on the survival of 24-h H/SD-exposed NMCMs were evaluated using different doses of 3-MA in MSC-treated NMCMs compared with MSC-treated NMCMs. Fluorescence staining with vital dyes calcein-AM shown in green indicates live cells, whereas ethidium homodimer-1 staining shown in red indicates the dead cells. The percentage of cell death was shown in (**right**; n=3 independent experiments). *P<0.05.

and III), were all significantly better in animals that were treated with MSCs (ie, the MI+MSC group) than in the absence of MSC administration (ie, in the MI group). Thus, the data indicate that MSC transplantation prevents cardiac cell death and hence improves the postinfarction left ventricular remodeling.

MSC Transplantation After MI Reduces Autophagic Flux in Cardiomyocytes

Autophagy-induced cell death has been recognized as an important modality of cell death. To investigate whether cardioprotection caused by MSCs was associated with autophagy modulation, we first assessed the autophagy-related protein level, LC3-II (microtubule-associated protein 1 light chain 3), and P62. Although the autophagosome marker LC3-II and the autophagy receptor P62 were significantly more and less abundant, respectively, in both MI and MI+MSC animals than in animals that underwent sham MI surgery (the Sham group), LC3-II levels were significantly lower, and P62 levels were significantly higher, in MI+MSC hearts than in MI hearts (Figure 1A and 1B). MI surgery was also associated with significant increases in the number of autophagosomes observed in transmission electron micrography images of cells from MI and MI+MSC hearts, but autophagosomes were significantly less common after treatment with MSCs than in cardiac cells from MI animals (Figure 1C and 1D), indicating inhibited autophagic process by MSC transplantation.

Because LC3-II is degraded when the autophagosome fuses with a lysosome to form an autolysosome,[21] the lower levels of LC3-II observed in MSC-treated animals could be caused by both a decline in the rate of autophagic degradation (ie, autophagic flux), if the rate of autophagosome synthesis drops faster than the rate of autophagosome/lysosome fusion, or an increase in autophagic flux, if the rate of autophagosome/lysosome fusion increases faster than the rate of autophagosome synthesis. To distinguish between these 2 states of autophagy processing, we evaluated the effect of MSC transplantation on autophagic flux by treating the animals with intraperitoneal injection of bafilomycin A1 (BafA1), which impedes autophagosome-lysosome fusion. BafA1 administration increased LC3-II levels in all 3 experimental groups (Sham, MI, and MI+MSC), but the magnitude of the increase was significantly lower in the MI+MSC and Sham groups than in MI animals (Figure 1E and 1F), which suggests that MSC therapy reduces the rate of autophagosome synthesis and, by extension, autophagic flux. Furthermore, we supplemented these results by conducting experiments in RFP-EGFP-LC3 transgenic mice under the control of a CAG promoter, which expresses a fluorescently tagged LC3 variant that produces a yellow signal in the high pH environment of autophagosomes (because both the RFP and EGFP moieties are active) and a red signal in the lower pH environment of autolysosomes (because EGFP fluorescence is quenched). Both autophagosomes and autolysosomes were significantly less common after treatment with MSCs than in cells from the MI group (Figure 1G and 1H). Collectively, these observations suggest that MSC transplantation leads to a significant decline in MI-induced autophagic flux after ischemic myocardial injury.

To further confirm whether autophagy inhibition contributes to cardioprotection and heart function improvement, we used 3-methyladenine (3-MA) to inhibit autophagy 30 minutes before MI and then assessed cardiomyocyte death and heart function. The changes of LC3-II associated with MSC transplantation were also observed when animals were treated with the autophagy inhibitor, 3-MA, 30 minutes before MI injury (Online Figure IIIA and IIIB). Terminal deoxynucleotidyl transferased deoxyuridine triphosphate nick-end labeling staining showed that 3-MA attenuated apoptotic myocyte death in ischemic border zone after 24 hours of ligation (Online Figure IIIC and IIID). Notably, 3-MA treatment resulted in better cardiac performance and improved ventricular remodeling compared with the MI group (Online Figure IIIE through IIIG). These results suggest that inhibition of autophagic flux can protect the cardiomyocyte and improve heart function after MI.

MSCs Inhibit Hypoxia and Serum Deprivation–Induced Autophagic Flux in Cultured Cardiomyocytes

The results from our initial observations in the murine MI model were corroborated in vitro by culturing neonatal mouse cardiomyocytes (NMCMs) with or without MSCs (NMCMs^{+MSCs} or NMCMs^{-MSCs}, respectively) under normoxic or hypoxic and serum deprivation (H/SD) conditions. H/SD increased NMCM LC3-II levels (Figure 2A and 2B), and it was further increased in the presence of BafA1, but measurements were significantly lower in NMCMs^{+MSCs} than in NMCMs^{-MSCs}. The magnitude of BafA1-induced LC3-II accumulation under H/SD conditions was also significantly lower in NMCMs cultured with rather than without MSCs (Figure 2B). Furthermore, we used a tandem fluorescence mRFP (mcherry red fluorescent protein)-GFP-LC3 reporter system to monitor the autophagic flux in NMCMs. Consistent with the data obtained from the in vivo study, a marked decrease in the number of both autophagosomes and autolysosomes was observed in NMCMs cocultured with MSCs (Figure 2D and 2E), which was further confirmed by transmission electron micrography examination (Figure 2C). Again, dose-dependent inhibition of autophagy by 3-MA significantly decreased cardiomyocyte death, which recapitulates the protective effects of MSCs coculture through inhibited autophagic activity (Figure 2F and 2G). Moreover, when the NMCMs^{+MSCs} were cultured with 1.25 to 2.5 mmol/L of the autophagy inhibitor 3-MA, H/SD-induced cell death was similar with NMCMs^{+MSCs}; however, when the NMCMs^{+MSCs} were cultured with 5 to 10 mmol/L of 3-MA, H/SD-induced cell death was significantly increased

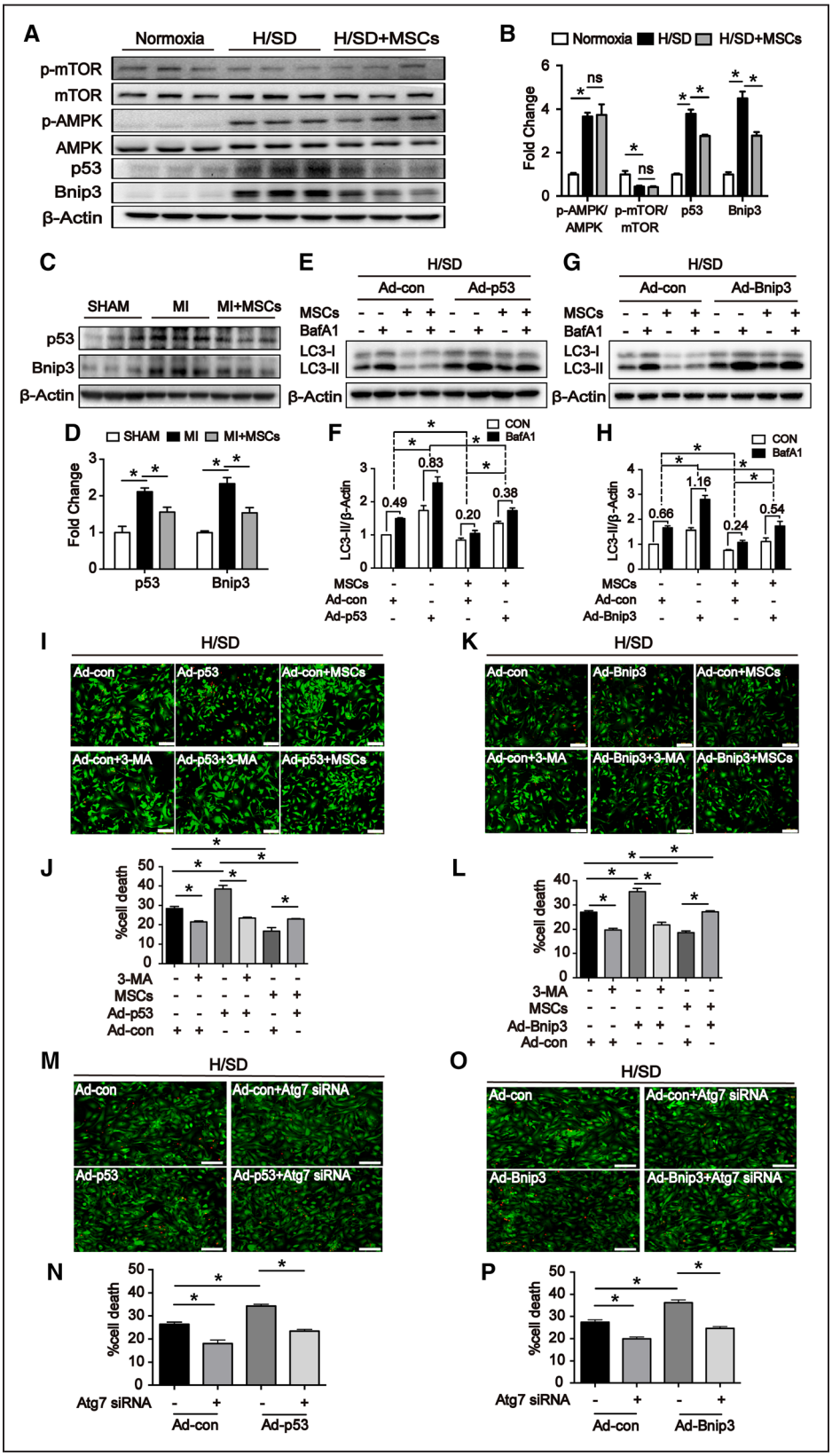

Figure 3. Both P53 and Bnip3 (B-cell lymphoma 2–interacting protein 3) induced by hypoxia in neonatal mouse cardiomyocytes (NMCMs) contribute to autophagy mediated cell death. A and **B**, p-AMPK (5′-adenosine monophosphate–activated protein kinase)/AMPK, p-mTOR/mTOR, p53, and Bnip3 levels were evaluated by Western blotting in NMCMs, and quantification is shown in the (**right**; n=3 independent experiments). **C** and **D**, Immunoblotting analysis for p53 and Bnip3 protein expression in mice (n=9) after 24-h ligation. Western blot analysis of protein lysates harvested from infarct border zone. Quantitative analysis of p53 and Bnip3 is shown in (**right**). **E** and **F**, NMCMs were infected with adenovirus for p53 overexpression (Ad-p53) and control (Ad-con), respectively, and the LC3-II (microtubule-associated protein 1 light chain 3) level was detected by Western blotting in 24-h hypoxia and serum deprivation (H/SD)–exposed (*Continued*)

Figure 3 Continued. NMCMs with or without mesenchymal stem cell (MSC) coculture, in the presence or absence of bafilomycin A1 (BafA1) (n=3 independent experiments). Quantification is shown in the (**right**). LC3-II expression levels both before and after BafA1 intervention were quantified, and their absolute changes (indicating autophagic flux) were calculated and analyzed by 1-way ANOVA shown in (**right**). **G** and **H**, NMCMs were infected with adenovirus for Bnip3 overexpression (Ad-Bnip3) and control (Ad-con), respectively, and the LC3-II levels were detected by Western blotting in 24-h H/SD-exposed NMCMs with or without MSC coculture, in the presence or absence of BafA1 (n=3 independent experiments). Quantification is shown in the (**right**). LC3-II expression levels both before and after BafA1 intervention were quantified, and their absolute changes (indicating autophagic flux) were calculated and analyzed by 1-way ANOVA shown in (**right**). **I** and **J**, NMCMs were treated with Ad-p53 or Ad-con (as controls) followed by exposure to H/SD for 24 h. The effects of MSC coculture were then evaluated by quantifying cell death using fluorescence staining using Calcein acetoxymethyl (Calcein-AM) vital dyes for live cells in green and ethidium homodimer-1 shown in red for dead cells (n=3 independent experiments; scale bar=100 μm). Quantitative analysis is shown in (**bottom**). **K** and **L**, NMCMs were treated with Ad-Bnip3 or Ad-con (as controls) followed by exposure to H/SD for 24 h. The effects of MSC coculture were then evaluated by quantifying cell death using fluorescence staining using calcein-AM vital dyes for live cells in green and ethidium homodimer-1 shown in red for dead cells (n=3 independent experiments; scale bar=100 μm). Quantitative analysis is shown in (**bottom**). **M**–**P**, NMCMs were treated with Ad-p53, Ad-Bnip3, or Ad-con (as controls) followed by exposure to H/SD for 24 h with or without Atg7 siRNA intervention (with the 50-nM concentration of siRNA). Cell death was then evaluated by using fluorescence staining using calcein-AM vital dyes for live cells in green and ethidium homodimer-1 shown in red for dead cells (n=3 independent experiments; scale bar=100 μm). **P*<0.05.

compared with NMCMs^{+MSCs}, indicating they act in the same way with MSCs to reduce the NMCM death and oversuppression of autophagy may be detrimental for NMCMs (Figure 2H and 2I). Thus, the decline in autophagic flux associated with MSC treatment after MI in vivo was also observed in NMCMs when the cells were cocultured with MSCs. To confirm our findings via a genetic approach, we transfected NMCMs with Atg7 siRNA, and the magnitude of BafA1-induced LC3-II accumulation under H/SD conditions was significantly lower in NMCMs transfected with Atg7 siRNA than negative control (NC; Online Figure IVA through IVD). Interestingly, H/SD-induced cell death was decreased when NMCMs transfected with 25- or 50-nM concentrations of Atg7 siRNA. However, a severe decrease in Atg7 expression failed to elicit any protection against H/SD-induced cell death (Online Figure IVE and IVF), suggesting that a moderate decrease in autophagy can confer a significant protection against H/SD-induced cell death obtained from NMCMs.

MSC-Induced Autophagic Modulation Is Mediated by p53 and Bnip3

To understand the mechanism by which MSC mediated the autophagy, we then investigated autophagy-related pathways. Autophagy is known to be regulated by at least 2 signaling pathways,[22] one involving mechanistic target of rapamycin and AMPK (5′-adenosine monophosphate–activated protein kinase)[23] and another that includes p53 and Bnip3 (B-cell lymphoma 2–interacting protein 3).[24–26] Mechanistic target of rapamycin and AMPK levels in H/SD-cultured NMCMs did not change significantly when the cells were cocultured with MSCs; therefore, it is likely that MSC-mediated autophagy inhibition was independent of mechanistic target of rapamycin and AMPK activity. Interestingly, both the mRNA and protein levels of p53 and Bnip3 were significantly increased in H/SD exposed cardiomyocytes compared with normal cultured ones, which were significantly decreased in MSC cocultured cardiomyocytes (Figure 3A and 3B; Online Figure VE), indicating that MSCs can modulate autophagy possibly through p53 and Bnip3 signaling. We next detected the expression of p53 and Bnip3 in vivo. Consistent with our in vitro data, both p53 and Bnip3 protein levels were increased in the border zone of MI mice, which were decreased in MSC-treated MI mice (Figure 3C and 3D), further confirming that these 2 signalings are involved in MSC therapy.

To further investigate the roles of p53 and Bnip3 in regulating autophagy in cardiomyocytes, we used 2 recombinant adenovirus that express full-length mouse p53 cDNA (Ad-p53) and Bnip3 cDNA (Ad-Bnip3). When NMCMs were transfected with adenoviruses containing murine Ad-p53, Ad-Bnip3, or control (Ad-con) cDNA, measures of BafA1-induced LC3-II accumulation (Figure 3E through 3H) were significantly greater in Ad-p53–transfected or Ad-Bnip3–transfected cells than in Ad-con–transfected cells under H/SD condition for 24 hours, and the enhanced autophagic flux by Ad-p53 or Ad-Bnip3 was also demonstrated by mRFP-GFP-LC3 fluorescence imaging (Online Figure VA and VB). The effects of BafA1 on LC3-II levels were also significantly lower when the Ad-p53–transfected, Ad-Bnip3–transfected, and Ad-con–transfected cells were cocultured with MSCs than in the absence of MSCs (Figure 3E through 3H). Although cell death increased significantly in response to p53 or Bnip3 overexpression, measurements declined significantly when Ad-p53–transfected, Ad-Bnip3–transfected, and Ad-con–transfected cells were cultured with, rather than without, MSCs or 3-MA (Figure 3I through 3L). However, the reduced autophagic flux and cell death by MSC coculture were partially abolished when overexpressing p53/Bnip3 in NMCMs compared with Ad-con–transfected cells (Figure 3E through 3L), suggesting p53 and Bnip3 were involved in the process of MSC-modulated autophagy. In addition, we further showed that the effects of BafA1 on LC3-II levels were also significantly lower when the Ad-p53–transfected, Ad-Bnip3–transfected, and Ad-con–transfected NMCMs were treated with Atg7 siRNA than NC (Online Figure VIA through VID), and cell death induced by p53 or Bnip3 overexpression was suppressed by Atg7 knockdown under H/SD conditions for 24 hours (Figure 3M through 3P). Thus, we demonstrate that inhibition of p53 or Bnip3 by MSC coculture confers protection against autophagy-induced cell death in H/SD-exposed NMCMs.

To determine the relationship between p53 and Bnip3, we assessed p53 and Bnip3 in NMCMs transfected with Ad-p53. Bnip3 protein and mRNA levels increased in response to p53 overexpression (Online Figure VIIA through VIIC). Furthermore, Bnip3 protein declined when p53 activity was downregulated in 24-hour H/SD-exposed NMCMs by transfecting the cells with p53 siRNA (Figure 4A and 4B). In contrast, siRNA-mediated declines in Bnip3 activity did not alter p53 protein levels (Figure 4C and 4D), even though either Bnip3 or p53 knockdown decreased the autophagic flux (Figure 4E through 4H). And vital staining of cells elucidated

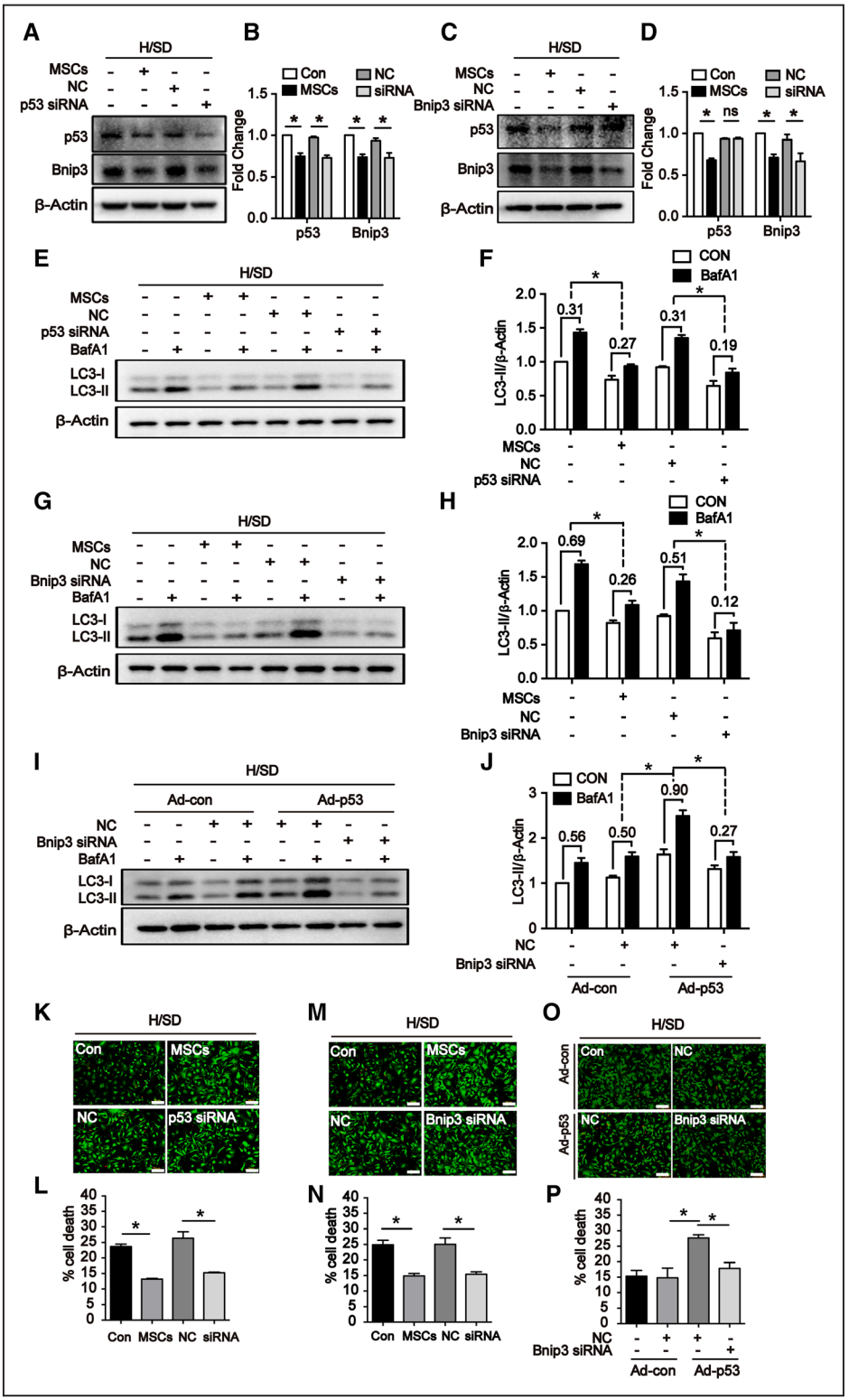

Figure 4. P53-mediated autophagy-induced cell death is Bnip3 (B-cell lymphoma 2–interacting protein 3) dependent. A and **B**, p53 and Bnip3 levels were detected by Western blotting in 24-h hypoxia and serum deprivation (H/SD)–exposed neonatal mouse cardiomyocytes (NMCMs) with or without p53 siRNA intervention (n=3 independent experiments). **C** and **D**, p53 and Bnip3 levels were detected by Western blotting in NMCMs with or without Bnip3 siRNA (n=3 independent experiments). **E** and **F**, LC3-II (microtubule-associated protein 1 light chain 3) levels were detected by Western blotting in 24-h H/SD-exposed NMCMs with and without p53 siRNA in the absence and presence of bafilomycin A1 (BafA1). Quantitative analysis of LC3-II is shown in (**right**). LC3-II expression levels both before and after BafA1 intervention were quantified, and their absolute changes (indicating autophagic flux) were calculated and analyzed by 1-way ANOVA shown in (**right**; n=3 independent experiments). **G** and **H**, LC3-II levels were detected by Western blotting in 24-h H/SD-exposed NMCMs with and without Bnip3 siRNA in the absence and presence of BafA1. Quantitative analysis of LC3-II is shown in (**right**). LC3-II expression levels both before and after BafA1 intervention were quantified, and their absolute changes (indicating autophagic flux) were calculated and analyzed by 1-way ANOVA shown in (**right**; n=3 independent experiments). **I** and **J**, Immunoblotting analysis for LC3-II protein in Ad-p53 transfected NMCMs with Bnip3 siRNA or without in the absence or presence of BafA1 under 24-h H/SD condition. Quantitative analysis of LC3-II is shown in (**right**). LC3-II expression levels both before and after BafA1 intervention were quantified, and their absolute changes (*Continued*)

Figure 4 Continued. (indicating autophagic flux) were calculated and analyzed by 1-way ANOVA shown in (**right**). **K** and **L**, Vital staining by fluorescence microscopy in 24-h H/SD-exposed NMCMs with and without p53 siRNA in 3 independent experiments (scale bar=100 μm). **M** and **N**, Vital staining by fluorescence microscopy in 24-h H/SD-exposed NMCMs with and without Bnip3 siRNA in 3 independent experiments (scale bar=100 μm). **O** and **P**, Vital staining by fluorescence microscopy in Ad-p53 transfected NMCMs with Bnip3 siRNA or without under 24-h H/SD condition (n=3 independent experiments; scale bar=100 μm). *P<0.05.

that p53 or Bnip3 knockdown induced reduction of autophagic flux of NMCMs accompanied with a significant decrease of cell death in H/SD conditions compared with NC (Figure 4K through 4N). Of note, Bnip3 downregulation abolished the increases in BafA1-induced LC3-II accumulation associated with p53 overexpression (Figure 4I and 4J) and H/SD-induced

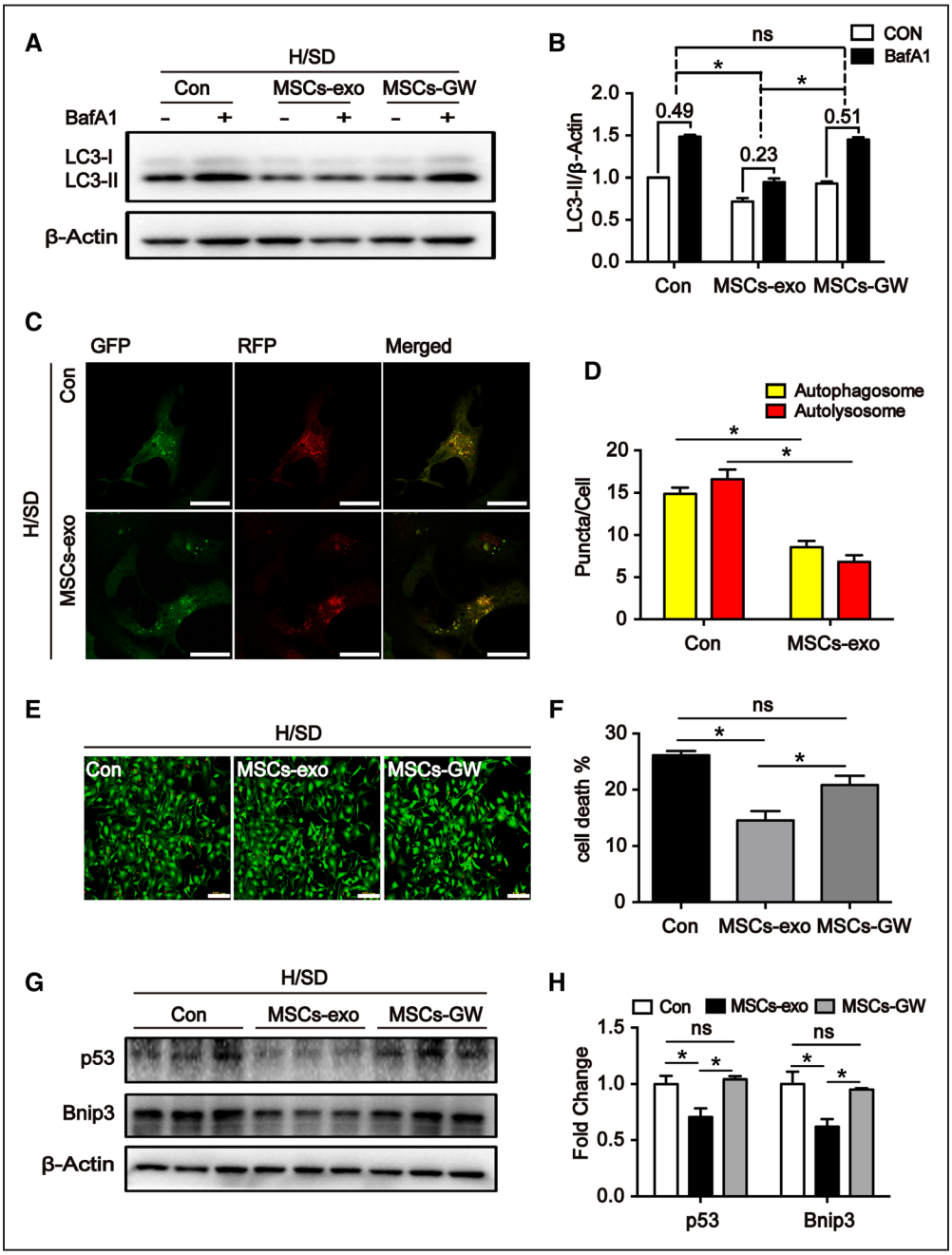

Figure 5. Mesenchymal stem cell–secreted exosomes (MSC-exo) regulate autophagic flux and enhance cell viability in neonatal mouse cardiomyocytes (NMCMs). A and **B**, LC3-II (microtubule-associated protein 1 light chain 3) was detected by Western blotting in NMCMs treated with MSC-exo, exosome obtained from mesenchymal stem cells that were given GW4869 (MSC-GW) in the presence or absence of bafilomycin A1 (BafA1) under 24-h hypoxia and serum deprivation (H/SD) conditions (n=3 independent experiments). Quantitative analysis of LC3-II is shown in (**right**). LC3-II expression levels both before and after BafA1 intervention were quantified, and their absolute changes (indicating autophagic flux) were calculated and analyzed by 1-way ANOVA shown in (**right**). **C** and **D**, Autophagosomes and autolysosomes were detected in 24-h H/SD-exposed NMCMs that expressed mRFP (mcherry red fluorescent protein)-GFP (green fluorescent protein)-LC3 after exosome therapy. Numbers of autophagosomes and autolysosomes in each cell (20–30 cells per group) were quantified (n=3 independent experiments; scale bar=25 μm). **E** and **F**, Vital staining by fluorescence microscopy for 24-h H/SD-exposed NMCMs that were treated with MSC-exo or MSC-GW (n=3 independent experiments; scale bar=100 μm). Quantitative analysis is shown in (**right**). **G** and **H**, P53 and Bnip3 (B-cell lymphoma 2–interacting protein 3) were also quantified by Western blotting in 24-h H/SD-exposed NMCM coincubation with MSC-exo or MSC-GW shown above (n=3 independent experiments). Quantitative analysis is shown in (**right**). *P<0.05.

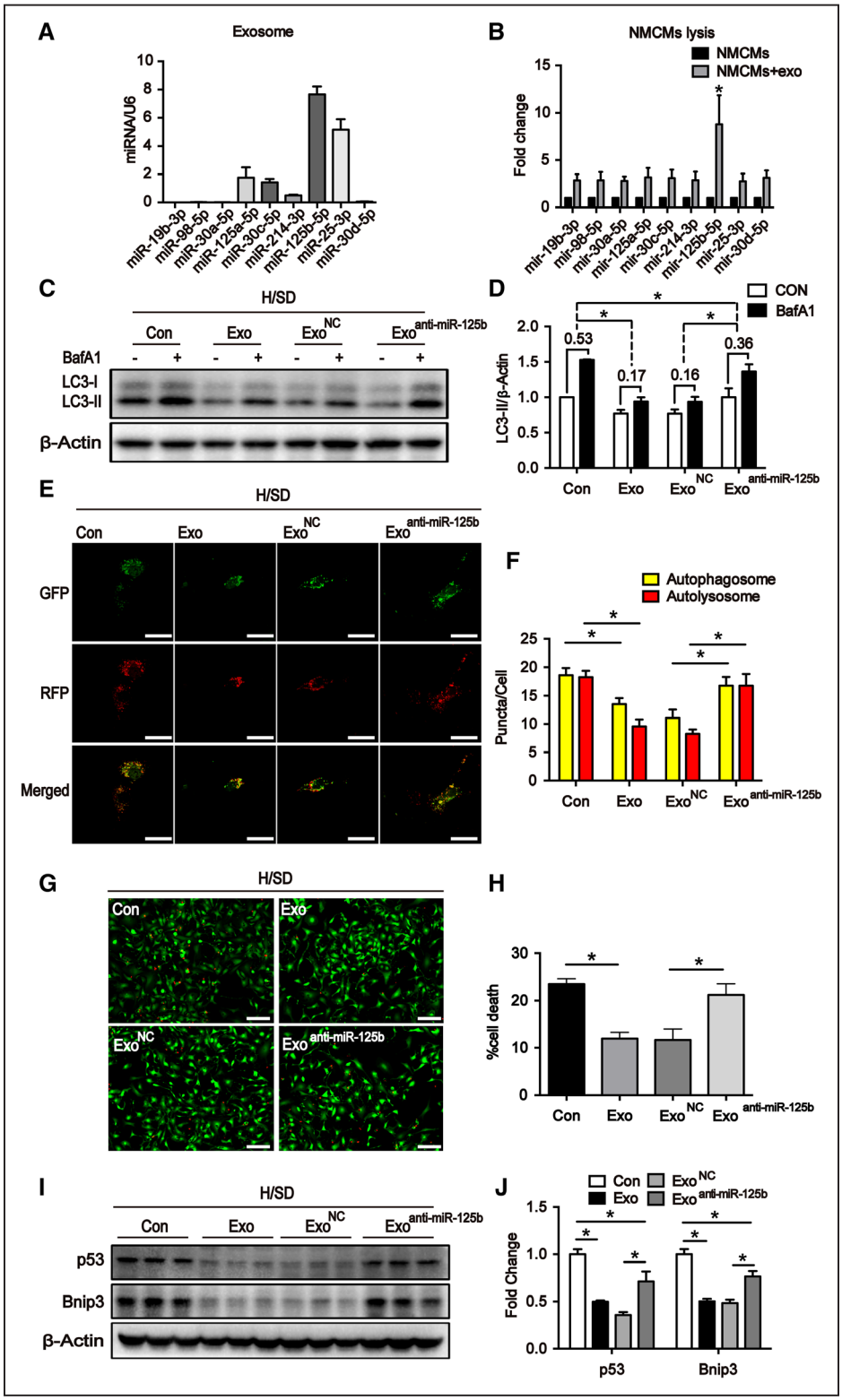

Figure 6. Loss of miR-125b-5p in mesenchymal stem cell–secreted exosome (MSC-exo) results in loss of its autophagy regulating and cardioprotective function in vitro. A, Polymerase chain reaction quantification of miRNA contents in the exosome obtained from mesenchymal stem cells (MSCs). **B**, Levels of cellular miR-125b-5p were the highest in neonatal mouse cardiomyocytes (NMCMs) treated with MSC-derived exosomes (n=3 independent experiments). **C** and **D**, Western blot identification for LC3-II (microtubule-associated protein 1 light chain 3) in NMCMs after incubation of different exosomes with or without bafilomycin A1 (BafA1) under 24-h hypoxia and serum deprivation (H/SD) condition. Exosomes were obtained from MSCs that were pretreated with anti-miR-125b-5p (MSC-exo$^{anti\text{-}miR\text{-}125b}$) or scramble (MSC-exo^{NC}). Quantitative analysis of LC3-II is shown in (**right**). LC3-II expression levels both before and after BafA1 intervention were quantified, and their absolute changes (indicating autophagic flux) were calculated and analyzed by 1-way ANOVA shown in (**right**; n=3 independent experiments). **E** and **F**, Autophagosomes and autolysosomes were detected in different exosome-treated NMCMs that expressed mRFP (mcherry red fluorescent protein)-GFP (green fluorescent protein)-LC3 under 24-h H/SD condition or H/SD condition without exosome (control [con]; scale bar=25 μm). **G** and **H**, (*Continued*)

Figure 6 Continued. Vital staining by fluorescence microscopy in NMCMs with or without different exosomes incubation under 24-h H/SD condition in 3 independent experiments. Quantitative analysis is shown in (**right**; scale bar=100 μm). **I** and **J**, Western blot identification for p53 and Bnip3 (B-cell lymphoma 2–interacting protein 3) in NMCMs after incubation of different exosomes as described above. Quantitative analysis of p53 and Bnip3 is shown in (**right**; n=3 independent experiments). NC indicates negative control. *P<0.05.

cell death was decreased in Ad-p53 transfected NMCMs by transfecting the cells with Bnip3 siRNA (Figure 4O and 4P), suggesting p53-mediated autophagy is Bnip3 dependent.

MSC-Secreted Exosomes Reduce Autophagic Flux in Cultured Cardiomyocytes

The MSC-secreted exosomes (MSC-exo) seem to have cardioprotective properties after MI,[5] thus, we investigated whether the decline in MI-induced autophagic flux associated with MSC transplantation may be at least partially mediated by MSC-exo. Exosomes were characterized by transmission electron micrography and by expression of the exosomal surface markers CD (cluster of differentiation) 63, Alix, and CD9 (Online Figure VIIIA and VIIIB), and exosomal uptake was verified via images of PKH26 fluorescence in NMCMs that had been cultured with PKH26-labeled exosomes under H/SD for 24 hours (Online Figure VIIIC).

The effects of exosome on autophagic flux of NMCMs were then evaluated. BafA1-induced LC3-II accumulation in H/SD-exposed NMCMs was significantly decreased by MSC-exo; however, these effects were abolished when treated with exosomes obtained from MSCs that were given GW4869—the exosome inhibitor (Figure 5A and 5B). Exosome production was inhibited by GW4869 in a dose-dependent manner, with complete blockage at a concentration of 20 μM (Online Figure VIIID). The effects of MSC-exo on autophagic flux of NMCMs were also associated with significant declines in autophagosome/autolysosome prevalence (Figure 5C and 5D). Accordingly, the reduction of autophagic flux induced by MSC-exo also resulted in much less cell death (Figure 5E and 5F). Importantly, incubation with MSC-exo did downregulate the expression level of p53 and Bnip3 in NMCMs induced by H/SD (Figure 5G and 5H; Online Figure VIIIE). Again, exosome obtained from MSCs treated with GW4869 failed to inhibit p53 and Bnip3 level induced by H/SD (Figure 5G and 5H). Thus, MSC-exo seems to have a key role in the antiautophagic activity of MSCs.

miR-125b-5p Is Abundant in MSC-Exo and Reduces Autophagic Flux in Cultured Cardiomyocytes

To further identify the components of exosomes that were responsible for MSC-exo regulating p53/Bnip3 autophagy signal pathway, we analyzed the exosomal miRNAs targeting the p53 gene. Of 9 exosomal miRNAs that are known to target p53 (miR-19b-3p, miR-98-5p, miR-30a-5p, miR-125a-5p, miR-30c-5p, miR-214-3p, miR-125b-5p, miR-25-3p, and miR-30d-5p),[27,28] the results from quantitative real-time polymerase chain reaction analyses indicated that miR-125b-5p was the most abundant in MSC-exo (Figure 6A) and increased most prominently during a 24-hour period in NMCMs that were cultured with MSC-exo (Figure 6B).

To confirm miR-125b-5p contributes to MSC-exo–mediated autophagy function, exosomes were obtained from MSCs that were pretreated with anti-miR-125b-5p oligonucleotide (MSC-exo$^{\text{anti-miR-125b}}$), with a scrambled as the control (MSC-exo$^{\text{NC}}$). The magnitude of BafA1-induced LC3-II accumulation under H/SD conditions was also significantly lower in NMCMs cultured with rather than without MSC-exo. However, these effects were abolished when treated with MSC-exo$^{\text{anti-miR-125b}}$ (Figure 6C and 6D). The similar results were observed in autophagosome/autolysosome prevalence (Figure 6E and 6F). Furthermore, MSC-exo$^{\text{anti-miR-125b}}$ failed to exert the effects on the autophagic flux of NMCMs, which were also reflected by no changes in the p53 and Bnip3 protein levels in H/SD exposed NMCMs compared with MSC-exo$^{\text{NC}}$ group (Figure 6I and 6J). As shown in Figure 6G and 6H, the protection against cell death by MSC-exo was abolished when treated with MSC-exo$^{\text{anti-miR-125b}}$.

To further validate the effects of miR-125b-5p on autophagy regulation, we tested the effects of the miR-125b-5p mimic or its inhibitor directly in NMCMs that were exposed to H/SD. Similar results were achieved when NMCMs were cultured with isolated miRNAs (ie, in the absence of exosomes). Transfected miR-125b-5p mimic directly into NMCMs recapitulated the inhibitive effects on autophagic flux compared with NC group (Online Figure IXA and IXB); whereas, transfection of its inhibitor exerted the opposite effects, exhibiting increased autophagic flux in NMCMs that were exposed to H/SD (Online Figure IXC and IXD). Being consistent with the autophagic flux, the levels of p53 and Bnip3 were decreased in response to treatment of miR-125b-5p mimic (Online Figure IXE, IXG, and IXM), whereas further enhanced when miR-125b-5p levels were manipulated in the reverse way (Online Figure IXF through IXH). Finally, miR-125b-5p mimic to NMCMs did offer protection against cell death under conditions of H/SD (Online Figure IXI and IXJ), whereas inhibition of miR-125b-5p further actually increased cell death of NMCMs exposed to H/SD (Online Figure IXK and IXL).

MSC-Exo Reduces Autophagic Flux When Injected Into Infarcted Hearts, and the Effect Is Dependent on miR-125b-5p

To confirm that the decline in autophagic flux associated with MSC transplantation is mediated by the exosomal delivery of miR-125b-5p, mice were injected with PBS, MSC-exo, MSC-exo that had been pretreated with anti-miR-125b-5p (MSC-exo$^{\text{anti-miR-125b}}$), or MSC-exo that had been pretreated with the control oligonucleotide (MSC-exo$^{\text{NC}}$) after surgically induced MI. After 24-hour ligation, BafA1-induced LC3-II accumulation in border zone of MI tissue was significantly lower in the MSC-exo group than in the PBS group; however, treating with MSC-exo$^{\text{anti-miR-125b}}$ failed to show similar effects on autophagic flux as MSC-exo or MSC-exo$^{\text{NC}}$ injection (Figure 7A and 7B). In addition, we also used CAG-RFP-EGFP-LC3 transgenic mice to monitor autophagic flux in vivo. In consistent with in vitro data, the prevalence of autophagosomes and autolysosomes was significantly lower in MSC-exo$^{\text{NC}}$ group than in

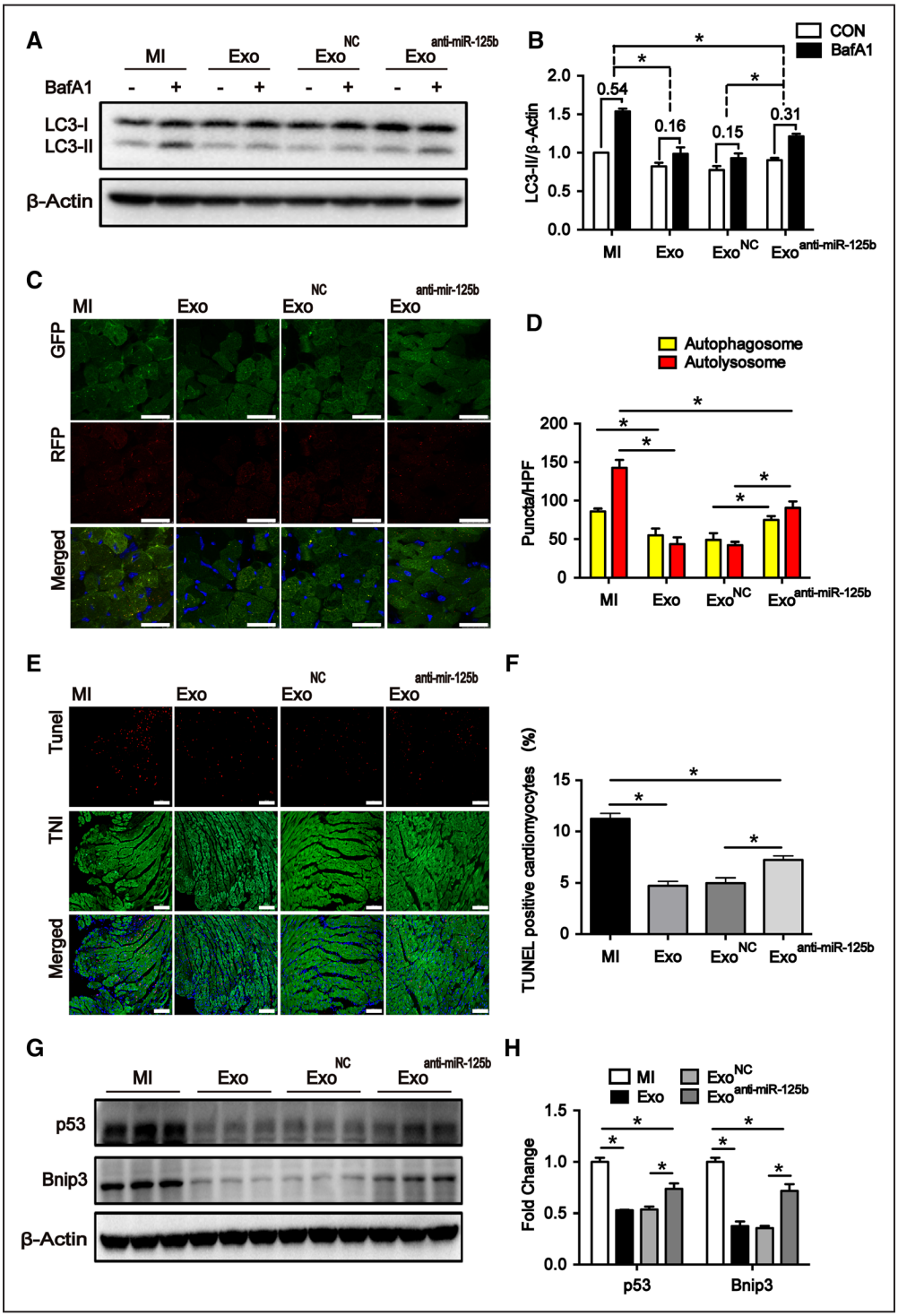

Figure 7. Loss of miR-125b-5p in mesenchymal stem cell–secreted exosome (MSC-exo) results in loss of its autophagy regulating and cardioprotective function in vivo. A and **B**, Autophagic flux was evaluated with bafilomycin A1 (BafA1) in coronary ligated mice that either received no therapy or exosome injection, including MSC-exo, MSC-exo^{NC}, and MSC-exo$^{anti\text{-}miR\text{-}125b\text{-}5p}$. Western blot analysis of protein lysates harvested from infarct border zone (n=6 per group). Quantitative analysis of LC3-II (microtubule-associated protein 1 light chain 3) is shown in (**right**). LC3-II expression levels both before and after BafA1 intervention were quantified, and their absolute changes (indicating autophagic flux) were calculated and analyzed by 1-way ANOVA shown in (**right**). **C** and **D**, Terminal deoxynucleotidyl transferased deoxyuridine triphosphate nick-end labeling (TUNEL)-positive cardiac myocytes in heart tissue of infract border zone for each group of mice as described above (scale bar=100 μm). Red, TUNEL-positive nuclei; blue, DAPI (4',6-diamidino-2-phenylindole, dihydrochloride)-stained nuclei; green, troponin-positive cardiac myocytes. Quantitative analysis of TUNEL-positive cells is shown in (**right**; n=6). **E** and **F**, Representative fluorescence images of heart tissue sections were obtained at 24 h after myocardial infarction (MI) in infract border zone from CAG (cytomegalovirus immediate early promoter enhancer with chicken beta-actin/rabbit beta-globin hybrid promoter)-RFP (red fluorescent protein)-EGFP (enhanced green fluorescent protein)-LC3 transgenic mice that were exposed to different exosome treatment. Autophagosome (yellow puncta) and autolysosome (red puncta) numbers in heart were calculated, respectively (n=3–4 per group with 4–5 microscopic fields per heart section analyzed; scale bar=25 μm). **G** and **H**, Western blot identification for p53/Bnip3 (B-cell lymphoma 2–interacting protein 3) pathway activation in heart tissue of infract border zone after different exosome treatments (n=9 per group). Quantitative analysis of p53 and Bnip3 is shown in (**right**). HPF indicates high-power field; and NC, negative control. *P<0.05.

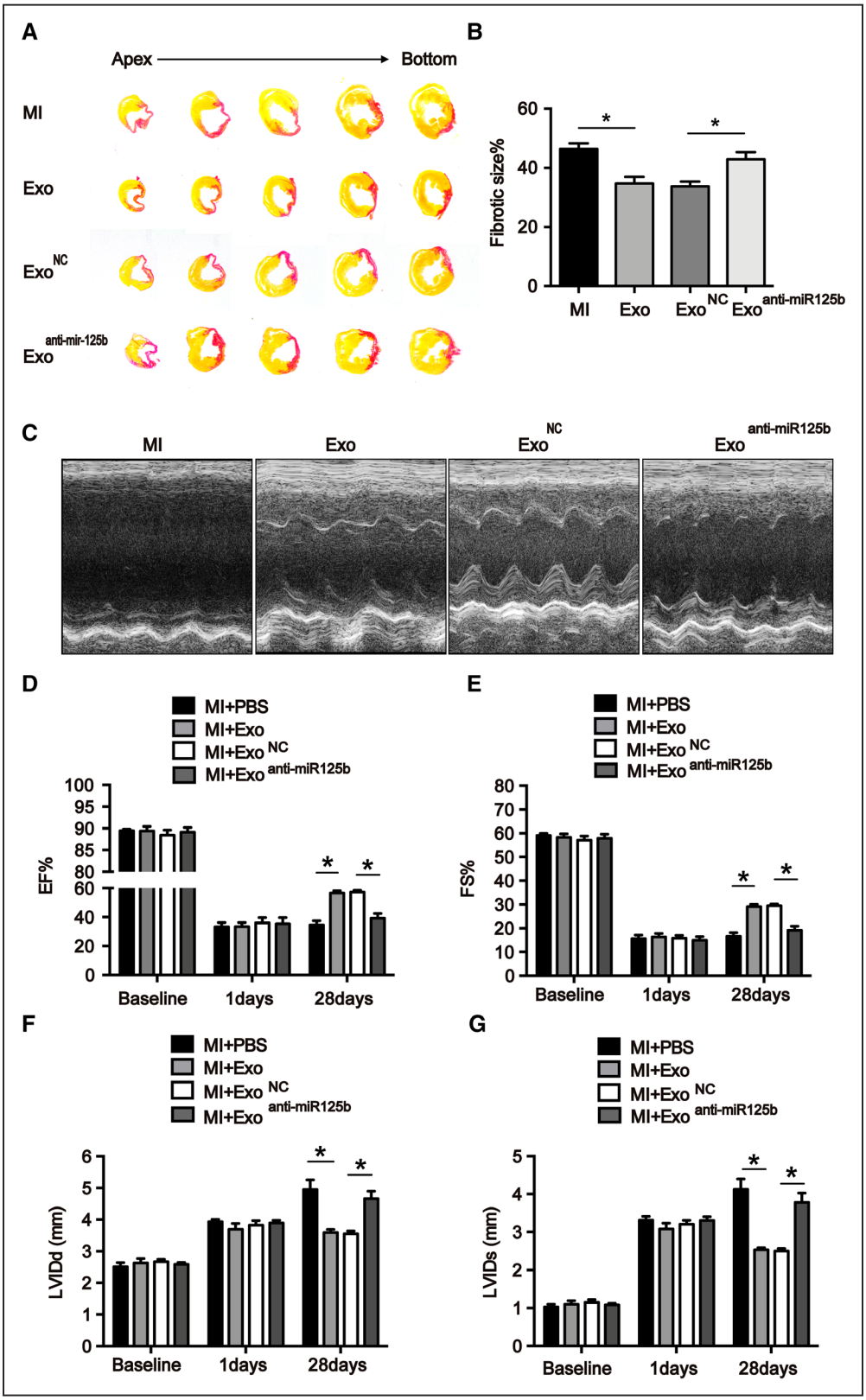

Figure 8. Loss of miR-125b-5p in mesenchymal stem cell (MSC)-derived exosomes results in poor improvement of cardiac function and infract size in vivo at 28 d after myocardial infarction (MI). A and **B**, Sirius Red staining was used to detect MI in hearts at 28 d postligation that either received no therapy or exosome injection, including mesenchymal stem cell–secreted exosome (MSC-exo), MSC-exo^{NC}, and MSC-exo$^{anti\text{-}miR\text{-}125b\text{-}5p}$. Percentage of fibrotic size in is shown in (**right**; n=7 per group). **C**–**G**, Representative photographs of M-mode echocardiography. Quantitative analysis of echocardiography (n=7 per group). EF indicates ejection fraction; FS, fractional shortening; LVEDD, left ventricular end-diastolic diameter; LVESD, left ventricular end-systolic diameter; and NC, negative control. *P<0.05.

MSC-exo$^{anti\text{-}miR\text{-}125b}$ group (Figure 7C and 7D). Terminal deoxynucleotidyl transferased deoxyuridine triphosphate nick-end labeling staining revealed that injection of exosomes could suppress cell death and MSC-exo$^{anti\text{-}miR\text{-}125b}$ abrogated cardioprotective function of MSCs (Figure 7E and 7F). Again, using Western blotting, we confirmed that p53 was the target of miR-125b-5p, which in turn modulated the expression level of Bnip3 (Figure 7G and 7H). Furthermore, the infarct size was significantly lower in the MSC-exo^{NC} group than in animals treated with MSC-exo$^{anti\text{-}miR\text{-}125b}$ (Figure 8A and 8B). Echocardiography also revealed that MSC-exo^{NC} group had better cardiac performance and improvement in ventricular remodeling compared with the MSC-exo$^{anti\text{-}miR\text{-}125b}$ group at 28 days after ligation (Figure 8C through 8G). Collectively, these observations indicate that the antiautophagic activity associated with MSC transplantation after MI is at least partially mediated by the exosomal transfer of miR-125b-5p.

Discussion

Basal levels of autophagy are essential for normal cardiomyocyte function,[22] and small increases in the basal rate may enable cardiac cells to maintain a sufficient supply of energy during mild conditions of ischemia, hypoxia, or nutrient deprivation.[14,29,30] However, if the ischemic event is more severe (as in acute MI and ischemia/reperfusion injury) or prolonged (as in chronic myocardial ischemia), the ensuing increase in autophagic flux may promote cell death,[14,31] exacerbate myocardial injury, and contribute to the progression of cardiac diseases, such as heart failure.[14,22,32] Although the cardioprotective paracrine activity of MSCs has been well documented, the findings presented in this report are the first to suggest that at least some of the benefits associated with MSC transplantation after MI can be attributed to the inhibition of ischemia-induced autophagy. We also demonstrate that the mechanism of MSC-induced autophagic inhibition involves the exosomal transfer of miR-125b-5p from MSCs to the native cells, where it interferes with p53/Bnip3 signaling.

Whether autophagy inhibits or induces cardiomyocyte death may depend on which distinct autophagy-related signaling pathways are activated. Multiple reports indicate that p53, which is known to have a crucial role in MI-induced cell death,[33,34] can both induce and inhibit autophagy,[26,35,36] and although Bnip3 is known to promote autophagy and cardiomyocyte death in response to ischemic and hypoxic injury,[24,37] it may have a cytoprotective role in some disease states.[38,39] Furthermore, the effect of p53 on Bnip3 expression appears to vary depending on the specific cell type or disease state being studied: p53 increased endogenous Bnip3 mRNA and protein levels, as well as autophagic flux and cell death, in cardiomyocytes[25] but had precisely the opposite effect on the expression of Bnip3 in HCT116 cells and of nip3a (the zebra fish homolog of mammalian Bnip3) in zebra fish.[40] In our study, both p53 and Bnip3 levels increased during hypoxia, and p53 overexpression increased the expression of Bnip3, leading to an increase in autophagic flux and cell death, whereas the p53-induced increase in cell death was abolished when the cells were cultured with MSCs or the autophagy inhibitor 3-MA. Although we found that p53 could partially induce autophagic cell death by Bnip3 after MI, we could not totally exclude the other potential roles of p53 that could also be involved in the protection conferred by MSC therapy; nevertheless, our study clearly shows that autophagy inhibition plays a critical role in MSC-based therapy for treating MI.

The role of exosomes in intracellular signaling, as well as their therapeutic potential for the treatment of myocardial disease,[5,8] has only recently become a prominent topic of research. Studies in a rat MI model have shown that MSC-exos have proangiogenic and anti-inflammatory properties,[5] whereas the results presented here suggest that they improve myocardial recovery by impeding autophagy. Our results also suggest that the key antiautophagic and cytoprotective component of the MSC exosomal cargo may be miR-125b-5p, which is one of several exosomal miRNAs known to target p53[27,28] and has been linked to a wide variety of biological processes, including anoikis in MSCs,[41] the hematopoietic output of stem cells,[42] the balance between stemness and differentiation in dermal stem cells,[43] and sepsis-induced cardiac dysfunction.[44]

In conclusion, the results presented here demonstrate the benefits associated with MSC transplantation after MI can be attributed to the inhibition of ischemia-induced autophagy, and the molecule responsible for autophagic inhibition, miR-125b-5p, interferes with p53/Bnip3 signaling. Furthermore, the miR-125b-5p is transferred to native cells via the uptake of MSC-exo. Collectively, these observations provide new insights into the mechanisms of cell-based therapy and may lead to the development of new therapeutic targets and strategies for the treatment of postinfarction left ventricular remodeling.

Sources of Funding

This work was supported by grants from the National Basic Research Program of China (973 program, No. 2014CB965100 for J. Wang and X. Hu), National Key Research and Development Program of China (No. 2017YFA 0103700 for X. Hu; No. 2016YFC1301204 for J. Wang), National Natural Science Foundation of China (No. 81320108003 and 31371498 for J. Wang; No. 81370247, 81622006, and 81670261 for X. Hu), and the Fundamental Research Funds for the Central Universities (No. 2016XZZX002-03 for X. Hu, No.BSF-001-00* for J. Wang).

Disclosures

None.

References

1. Williams AR, Hare JM. Mesenchymal stem cells: biology, pathophysiology, translational findings, and therapeutic implications for cardiac disease. *Circ Res*. 2011;109:923–940. doi: 10.1161/CIRCRESAHA.111.243147.
2. Hu X, Xu Y, Zhong Z, et al. A large-scale investigation of hypoxia-preconditioned allogeneic mesenchymal stem cells for myocardial repair in nonhuman primates: paracrine activity without remuscularization. *Circ Res*. 2016;118:970–983. doi: 10.1161/CIRCRESAHA.115.307516.
3. Arslan F, Lai RC, Smeets MB, Akeroyd L, Choo A, Aguor EN, Timmers L, van Rijen HV, Doevendans PA, Pasterkamp G, Lim SK, de Kleijn DP. Mesenchymal stem cell-derived exosomes increase ATP levels, decrease oxidative stress and activate PI3K/Akt pathway to enhance myocardial viability and prevent adverse remodeling after myocardial ischemia/reperfusion injury. *Stem Cell Res*. 2013;10:301–312. doi: 10.1016/j.scr.2013.01.002.
4. Bian S, Zhang L, Duan L, Wang X, Min Y, Yu H. Extracellular vesicles derived from human bone marrow mesenchymal stem cells promote angiogenesis in a rat myocardial infarction model. *J Mol Med (Berl)*. 2014;92:387–397. doi: 10.1007/s00109-013-1110-5.
5. Teng X, Chen L, Chen W, Yang J, Yang Z, Shen Z. Mesenchymal stem cell-derived exosomes improve the microenvironment of infarcted

myocardium contributing to angiogenesis and anti-inflammation. *Cell Physiol Biochem*. 2015;37:2415–2424. doi: 10.1159/000438594.
6. Timmers L, Lim SK, Arslan F, Armstrong JS, Hoefer IE, Doevendans PA, Piek JJ, El Oakley RM, Choo A, Lee CN, Pasterkamp G, de Kleijn DP. Reduction of myocardial infarct size by human mesenchymal stem cell conditioned medium. *Stem Cell Res*. 2007;1:129–137. doi: 10.1016/j.scr.2008.02.002.
7. Yu B, Kim HW, Gong M, Wang J, Millard RW, Wang Y, Ashraf M, Xu M. Exosomes secreted from GATA-4 overexpressing mesenchymal stem cells serve as a reservoir of anti-apoptotic microRNAs for cardioprotection. *Int J Cardiol*. 2015;182:349–360. doi: 10.1016/j.ijcard.2014.12.043.
8. Phinney DG, Pittenger MF. Concise review: MSC-derived exosomes for cell-free therapy. *Stem Cells*. 2017;35:851–858. doi: 10.1002/stem.2575.
9. Valadi H, Ekström K, Bossios A, Sjöstrand M, Lee JJ, Lötvall JO. Exosome-mediated transfer of mRNAs and microRNAs is a novel mechanism of genetic exchange between cells. *Nat Cell Biol*. 2007;9:654–659. doi: 10.1038/ncb1596.
10. Boulanger CM, Loyer X, Rautou PE, Amabile N. Extracellular vesicles in coronary artery disease. *Nat Rev Cardiol*. 2017;14:259–272. doi: 10.1038/nrcardio.2017.7.
11. Cuervo AM. Autophagy: many paths to the same end. *Mol Cell Biochem*. 2004;263:55–72.
12. Levine B, Kroemer G. Autophagy in the pathogenesis of disease. *Cell*. 2008;132:27–42. doi: 10.1016/j.cell.2007.12.018.
13. Mizushima N, Levine B, Cuervo AM, Klionsky DJ. Autophagy fights disease through cellular self-digestion. *Nature*. 2008;451:1069–1075. doi: 10.1038/nature06639.
14. Matsui Y, Takagi H, Qu X, Abdellatif M, Sakoda H, Asano T, Levine B, Sadoshima J. Distinct roles of autophagy in the heart during ischemia and reperfusion: roles of AMP-activated protein kinase and Beclin 1 in mediating autophagy. *Circ Res*. 2007;100:914–922. doi: 10.1161/01.RES.0000261924.76669.36.
15. Buss SJ, Riffel JH, Katus HA, Hardt SE. Augmentation of autophagy by mTOR-inhibition in myocardial infarction: when size matters. *Autophagy*. 2010;6:304–306.
16. Kanamori H, Takemura G, Goto K, et al. Autophagy limits acute myocardial infarction induced by permanent coronary artery occlusion. *Am J Physiol Heart Circ Physiol*. 2011;300:H2261–H2271. doi: 10.1152/ajpheart.01056.2010.
17. Nah J, Fernández ÁF, Kitsis RN, Levine B, Sadoshima J. Does autophagy mediate cardiac myocyte death during stress? *Circ Res*. 2016;119:893–895. doi: 10.1161/CIRCRESAHA.116.309765.
18. Denton D, Nicolson S, Kumar S. Cell death by autophagy: facts and apparent artefacts. *Cell Death Differ*. 2012;19:87–95. doi: 10.1038/cdd.2011.146.
19. Gao T, Zhang SP, Wang JF, Liu L, Wang Y, Cao ZY, Hu QK, Yuan WJ, Lin L. TLR3 contributes to persistent autophagy and heart failure in mice after myocardial infarction. *J Cell Mol Med*. 2018;22:395–408. doi: 10.1111/jcmm.13328.
20. Hu X, Wu R, Jiang Z, et al. Leptin signaling is required for augmented therapeutic properties of mesenchymal stem cells conferred by hypoxia preconditioning. *Stem Cells*. 2014;32:2702–2713. doi: 10.1002/stem.1784.
21. Klionsky DJ, Abdelmohsen K, Abe A, al. e. Guidelines for the use and interpretation of assays for monitoring autophagy (3rd edition). *Autophagy*. 2016;12:1–222.
22. Lavandero S, Troncoso R, Rothermel BA, Martinet W, Sadoshima J, Hill JA. Cardiovascular autophagy: concepts, controversies, and perspectives. *Autophagy*. 2013;9:1455–1466. doi: 10.4161/auto.25969.
23. Kim J, Kundu M, Viollet B, Guan KL. AMPK and mTOR regulate autophagy through direct phosphorylation of Ulk1. *Nat Cell Biol*. 2011;13:132–141. doi: 10.1038/ncb2152.
24. Azad MB, Chen Y, Henson ES, Cizeau J, McMillan-Ward E, Israels SJ, Gibson SB. Hypoxia induces autophagic cell death in apoptosis-competent cells through a mechanism involving BNIP3. *Autophagy*. 2008;4:195–204.
25. Wang EY, Gang H, Aviv Y, Dhingra R, Margulets V, Kirshenbaum LA. p53 mediates autophagy and cell death by a mechanism contingent on Bnip3. *Hypertension*. 2013;62:70–77. doi: 10.1161/HYPERTENSIONAHA.113.01028.
26. White E. Autophagy and p53. *Cold Spring Harb Perspect Med*. 2016;6:a026120. doi: 10.1101/cshperspect.a026120.
27. Hünten S, Siemens H, Kaller M, Hermeking H. The p53/microRNA network in cancer: experimental and bioinformatics approaches. *Adv Exp Med Biol*. 2013;774:77–101. doi: 10.1007/978-94-007-5590-1_5.
28. Hermeking H. MicroRNAs in the p53 network: micromanagement of tumour suppression. *Nat Rev Cancer*. 2012;12:613–626. doi: 10.1038/nrc3318.
29. Gustafsson AB, Gottlieb RA. Autophagy in ischemic heart disease. *Circ Res*. 2009;104:150–158. doi: 10.1161/CIRCRESAHA.108.187427.
30. Yan L, Vatner DE, Kim SJ, Ge H, Masurekar M, Massover WH, Yang G, Matsui Y, Sadoshima J, Vatner SF. Autophagy in chronically ischemic myocardium. *Proc Natl Acad Sci USA*. 2005;102:13807–13812. doi: 10.1073/pnas.0506843102.
31. Takagi H, Matsui Y, Hirotani S, Sakoda H, Asano T, Sadoshima J. AMPK mediates autophagy during myocardial ischemia in vivo. *Autophagy*. 2007;3:405–407.
32. Zhu H, Tannous P, Johnstone JL, Kong Y, Shelton JM, Richardson JA, Le V, Levine B, Rothermel BA, Hill JA. Cardiac autophagy is a maladaptive response to hemodynamic stress. *J Clin Invest*. 2007;117:1782–1793. doi: 10.1172/JCI27523.
33. Bialik S, Geenen DL, Sasson IE, Cheng R, Horner JW, Evans SM, Lord EM, Koch CJ, Kitsis RN. Myocyte apoptosis during acute myocardial infarction in the mouse localizes to hypoxic regions but occurs independently of p53. *J Clin Invest*. 1997;100:1363–1372. doi: 10.1172/JCI119656.
34. Long X, Boluyt MO, Hipolito ML, Lundberg MS, Zheng JS, O'Neill L, Cirielli C, Lakatta EG, Crow MT. p53 and the hypoxia-induced apoptosis of cultured neonatal rat cardiac myocytes. *J Clin Invest*. 1997;99:2635–2643. doi: 10.1172/JCI119452.
35. Crighton D, Wilkinson S, Ryan KM. DRAM links autophagy to p53 and programmed cell death. *Autophagy*. 2007;3:72–74.
36. Zhang XD, Wang Y, Wang Y, Zhang X, Han R, Wu JC, Liang ZQ, Gu ZL, Han F, Fukunaga K, Qin ZH. p53 mediates mitochondria dysfunction-triggered autophagy activation and cell death in rat striatum. *Autophagy*. 2009;5:339–350.
37. Regula KM, Ens K, Kirshenbaum LA. Inducible expression of BNIP3 provokes mitochondrial defects and hypoxia-mediated cell death of ventricular myocytes. *Circ Res*. 2002;91:226–231.
38. Bellot G, Garcia-Medina R, Gounon P, Chiche J, Roux D, Pouysségur J, Mazure NM. Hypoxia-induced autophagy is mediated through hypoxia-inducible factor induction of BNIP3 and BNIP3L via their BH3 domains. *Mol Cell Biol*. 2009;29:2570–2581. doi: 10.1128/MCB.00166-09.
39. Hamacher-Brady A, Brady NR, Logue SE, Sayen MR, Jinno M, Kirshenbaum LA, Gottlieb RA, Gustafsson AB. Response to myocardial ischemia/reperfusion injury involves Bnip3 and autophagy. *Cell Death Differ*. 2007;14:146–157. doi: 10.1038/sj.cdd.4401936.
40. Feng X, Liu X, Zhang W, Xiao W. p53 directly suppresses BNIP3 expression to protect against hypoxia-induced cell death. *EMBO J*. 2011;30:3397–3415. doi: 10.1038/emboj.2011.248.
41. Yu X, Cohen DM, Chen CS. miR-125b Is an adhesion-regulated microRNA that protects mesenchymal stem cells from anoikis. *Stem Cells*. 2012;30:956–964. doi: 10.1002/stem.1064.
42. O'Connell RM, Chaudhuri AA, Rao DS, Gibson WS, Balazs AB, Baltimore D. MicroRNAs enriched in hematopoietic stem cells differentially regulate long-term hematopoietic output. *Proc Natl Acad Sci USA*. 2010;107:14235–14240. doi: 10.1073/pnas.1009798107.
43. Zhang L, Stokes N, Polak L, Fuchs E. Specific microRNAs are preferentially expressed by skin stem cells to balance self-renewal and early lineage commitment. *Cell Stem Cell*. 2011;8:294–308. doi: 10.1016/j.stem.2011.01.014.
44. Ma H, Wang X, Ha T, Gao M, Liu L, Wang R, Yu K, Kalbfleisch JH, Kao RL, Williams DL, Li C. MicroRNA-125b prevents cardiac dysfunction in polymicrobial sepsis by targeting TRAF6-mediated nuclear factor κB activation and p53-mediated apoptotic signaling. *J Infect Dis*. 2016;214:1773–1783. doi: 10.1093/infdis/jiw449.